Acta Neuropathol (Berl) (1984) 64:53–60

Acta Neuropathologica

Ultrastructural Studies on the Pathogenesis of Poliomyelitis in Monkeys Infected with Poliovirus

I. Hashimoto[1], A. Hagiwara[2], and T. Komatsu[2]

Depts. of [1] Pathology and [2] Enteroviruses, National Institute of Health, Murayama Annex, Gakuen, Musashimurayam, Tokyo 190-12, Japan

Summary. Poliovirus was inoculated intraspinally into cynomolgus monkeys to determine whether nerve cell damage in the central nervous system (CNS) is due primarily to virus multiplication in the neuron or to secondary effects of virus multiplication in the supporting cells. Electron-microscopically, the development of cytopathogenesis and of membrane-bound vesicles and virus particles in the neurons of the CNS in monkeys infected with poliovirus was compared with that of infected cultured cynomolgus monkey kidney (CMK) cells. The structure of membrane-bound vesicles in cytoplasm of damaged motoneuron was examined and found to be similar to the vesicles in infected cultured CMK cells. Virus-like particles were detected occasionally around or within membrane-bound vesicles in the cytoplasm of degenerating motoneurons as well as cultured CMK cells, although intracytoplasmic crystals were not detected in the neuron. No virus particles or membrane-bound vesicles were found in astrocyte foot plates, microglia, oligodendrocytes, axons, vascular endothelial, and inflammatory cells. In addition, poliovirus antigen was detected only in the nerve cells of the CNS by the immunoperoxidase technique, although specific staining was never found in the supporting tissues. From the present results we suggest that membrane-bound vesicles in the cytoplasm of the motoneuron are closely correlated with virus multiplication and that damage of the nerve cell is due to the direct action of the poliovirus.

Key words: Poliomyelitis – Poliovirus – Monkeys – Pathogenesis

Introduction

In human poliomyelitis caused by poliovirus, there has been discussion as to whether the nerve cell damage is due primarily to virus multiplication in the neurons or to secondary effects of virus multiplication in the supporting cells of the central nervous system (CNS). Electron-microscopically, virus-like particles in the necrotizing motoneuron of the CNS of monkeys infected with poliovirus were detected first by Bodian (1964). He indicated that nerve cell damage is due to the direct action of virus multiplication. However, there remains the suspicion that poliovirus particles were found in the neuron. In contrast, Simon et al. (1970) reported that specific immunofluorescence was not detected in any of the neurons in the CNS of monkeys infected with poliovirus, although virus antigen was detected in the vascular endothelial and mononuclear inflammatory cells. They inferred, therefore, that it is related either to involvement of the nerve cell by the inflammatory response or to involvement of the astrocyte foot plates and capillary endothelium.

In the present investigation, poliovirus was inoculated intraspinally into cynomolgus monkeys to determine whether the nerve cell damage in the CNS is due primarily to virus multiplication in the neuron or secondary to the effects of virus multiplication in the supporting cells of the CNS. Electron-microscopically, the development of cytopathogenesis and membrane-bound vesicles and virus particles in the neurons of the CNS in monkeys infected with poliovirus were compared with those of infected cultured kidney cells of the cynomolgus monkeys. In addition, a light-microscopic immunoperoxidase study was undertaken to determine whether poliovirus antigen is detected only in the nerve cells.

Offprint requests to: I. Hashimoto, MD (address see above)

Materials and Methods

Virus

The Mahoney strain of poliovirus was used in the experiment. Monolayers of cultured cynomolgus monkey kidney (CMK) cells were infected with an appropriately diluted virus suspension (ca. 0.1 PFU/cell), and the cultures were harvested when the cytopatho-

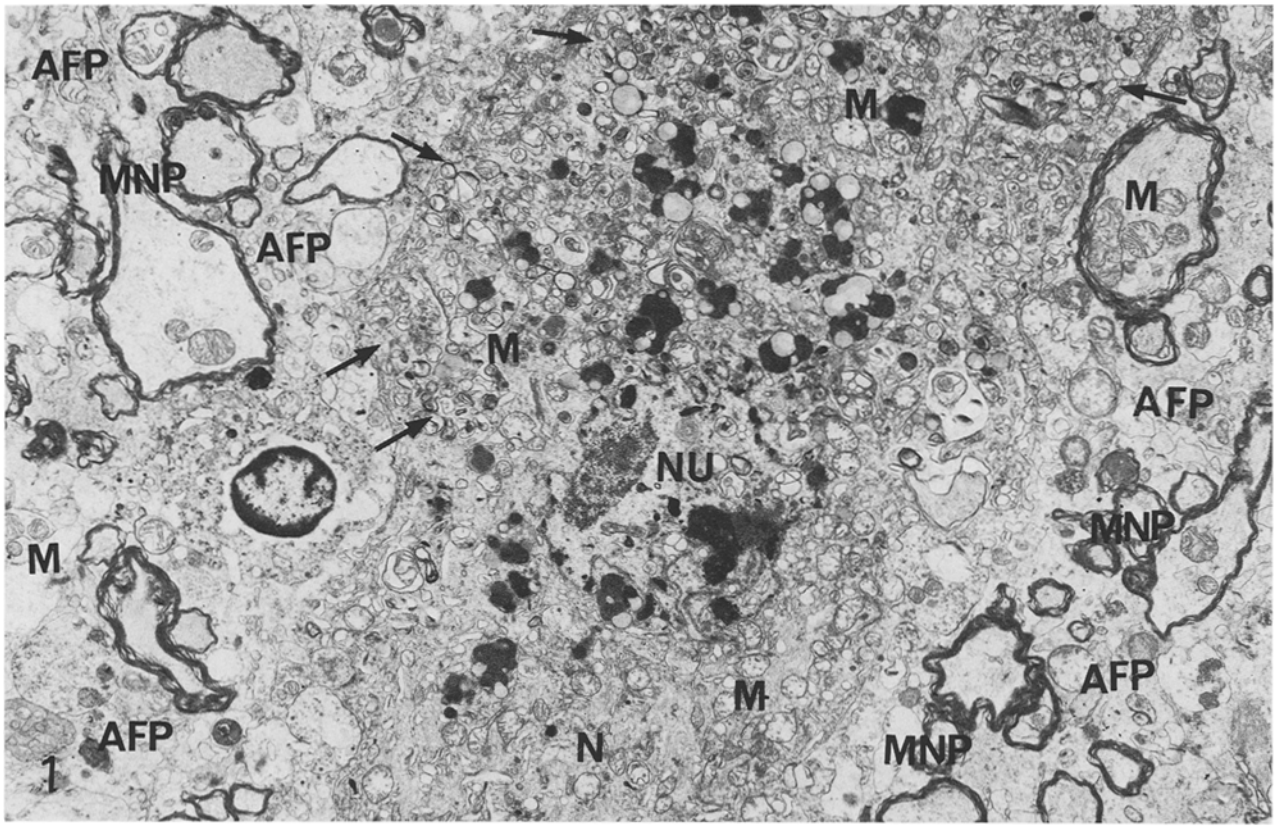

Fig. 1. A degenerating motoneuron (*N*) in the lumbar cord on day 2. Numerous cytoplasmic membrane-bound vesicles (*arrows*), degeneration or destruction of mitochondria (*M*), nuclear (*NU*) degeneration, and disappearance of Nissl substance in a neuron. Note no abnormalities of astrocyte foot plates (*AFP*) and myelinated nerve processes (*MNP*) around a degenerating motoneuron. × 6,500

genic effect was maximal. The harvest was frozen and thawed five times at 10 MHz for 5 min and then centrifuged at 3,000 rpm for 10 min. The supernate was concentrated by polyethylene glycal and centrifuged through sucrose (30% w/w) solution at 39,000 rpm for 3 h. The virus was purified by density gradient centrifugation of CsCl and further purified by sucrose density gradient (15–30% w/w) and CsCl density gradient centrifugation.

Monkeys

Healthy cynomolgus monkeys (*Macaca irus*), 1.8–3.1 kg b.w., imported from Malaysia were used after a 9-week quarantine. Each monkey was kept in a separate cage and fed a solid diet of sweet potatoes, apples, lemon, and water.

Inoculation into Monkeys

Four monkeys were inoculated into the lumbar spinal cord with 0.1 ml of a suspension containing $10^{6.5}$ $TCID_{50}$ of purified virus of the Mahoney strain.

Clinical Observations

The inoculated monkeys were examined daily for 3 days.

Histopathologic Studies

Samples of the CNS were fixed in 10% neutral formalin: ten to 20 samples from the lumbar cord enlargement at 1 mm intervals, six from the cervical cord enlargement, two from the medulla oblongata, and one from the mid-brain. They were sectioned at 5 μm after embedding in paraffin. The sections were stained by hematoxylin and eosin (HE), gallocyanin, and Luxol fast blue.

Cell Cultures

Continuous line CMK cell monolayers were grown to confluency in prescription bottles in Eagle's minimum essential medium (MEM) with 10% calf serum and maintained in MEM with 2% calf serum.

Inoculation into Cultured CMK Cells

The CMK cell monolayer in the prescription bottle was drained and infected with 0.2 ml of virus suspension which contained 10 plaque-forming units (PFU) of virus per 0.1 ml. The virus was allowed to adsorb to cells for 1 h at 37° C and thereafter was covered with 5 ml of MEM and incubated at 37° C.

Electron-microscopic Technique

In Vivo. One monkey under deep anesthesia with Nembutal sodium was killed at 8 h, 1, 2 and 3 days after inoculation. Pieces of approximately 2 mm^3 from the CNS of these monkeys were fixed in 2% glutaraldehyde in 0.2 M cacodylate-buffered solution for 20 min and postfixed in 1% osmium tetroxide in the same buffered solution for 40 min, treated with 20% uranyl acetate and rapidly dehydrated in ethanol series, and embedded in Epon. Specimens of the lumbar cord did not contain traumatic lesions caused by injection.

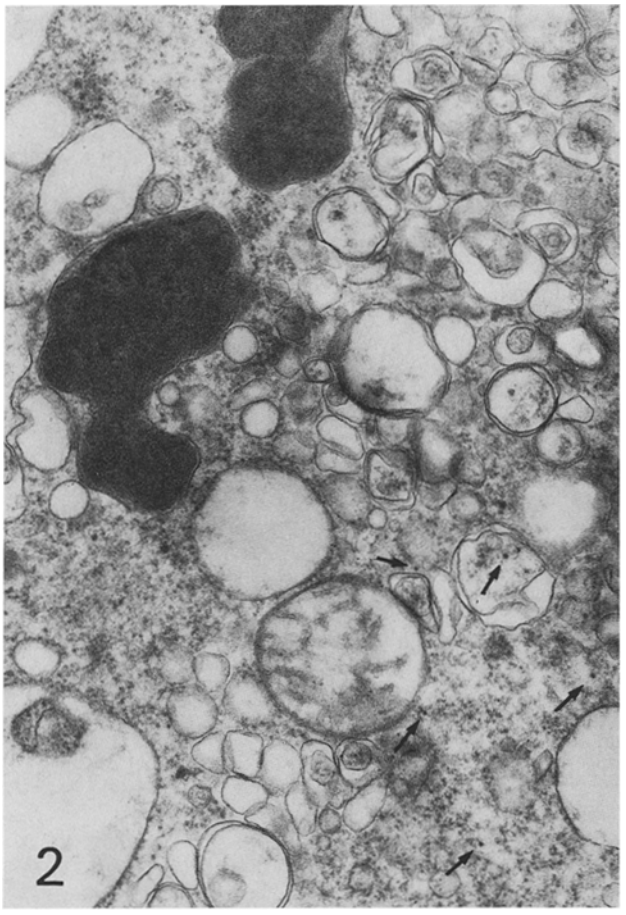

Fig. 2. Higher magnification of cytoplasmic membrane-bound vesicles in Fig. 1. Note virus-like particles (*arrows*) within or around the vesicles. × 32,000

In Vitro. Four, 5, 6, 7, 8, 10, and 24 h after inoculation, the CMK cell monolayers infected with poliovirus in prescription bottles were washed once with phosphate-buffered solution (PBS) and fixed in 2% glutaraldehyde in 0.2% cacodylate-buffered solution for 40 min. The cells were then scraped off the glass surface with a rubber policeman and centrifuged at 1,000 rpm for 15 min; the pellet was stained with 2% uranyl acetate, then rapidly dehydrated in an ethanol series, and embedded in Epon.

Ultrathin sections of the CNS and cultured CMK cells were cut by an LKB-ultramicrotome equipped with a diamond knife and mounted on 200-mesh copper grids, stained with lead citrate, and examined in a JEM-100 CX electron microscope.

Immunoperoxidase Technique

The indirect immunoperoxidase technique used was essentially the same as that described by Nakane and Pierce (1967) and McLean and Nakane (1974). Indirect peroxidase antibody staining was done using rabbit anti-poliovirus hyperimmune serum prepared in the rabbit. Peroxidase-conjugated anti-rabbit gamma-globulin was obtained from E.Y. Laboratories (USA). Immediately after necropsy, the lumbar and cervical cords, pons, and thalamus of the monkeys were fixed overnight at 4° C for light microscopy with periodate-lysin paraformaldehyde (PLP) fixative, embedded in Ames O.C.T. compound, frozen quickly, and sectioned. Endogenous peroxidase activity was blocked with 0.3% hydrogen peroxide in 100% methanol for 20 min at room temperature. The sections were treated with anti-poliovirus rabbit serum for 1 h at room temperature, washed in PBS for 15 min, and then stained with peroxidase-conjugated anti-rabbit gamma-globulin in a moist chamber for 30 min at room temperature and rinsed in PBS for 15 min. The sections were stained with 0.005% 3,3′-diaminobenzidine tetrahydrochloride (DAB) in a moist chamber for 5 min at room temperature and rinsed in PBS for 15 min. The stained sections were mounted on Eukitt.

The specificity of the anti-poliovirus rabbit serum was established by indirect peroxidase antibody staining of the lumbar and cervical cords of monkeys or CMK cell infected with poliovirus, and a negative reaction with the lumbar and cervical cords of enterovirus 71-infected monkeys or uninfected CMK cells. The specificity of anti-poliovirus rabbit serum was also established by a negative reaction with the lumbar and cervical cords of poliovirus-infected monkeys treated with normal rabbit serum prior to infection with poliovirus.

Results

Clinical Findings

No clinical symptoms were found in two monkeys killed at 8 h and 1 day after inoculation. On days 2 and 3, however, two monkeys showed complete paralysis of the lower or upper extremities.

Light-microscopic Findings

The CNS lesions were observed in all four monkeys inoculated with poliovirus. After 8 h, chromatolysis, degeneration and necrosis of the neurons, neuronophagia, gliosis, interstitial inflammatory reaction, and meningeal inflammatory cell infiltration were observed in the lumbar cord only. On days 1 – 3, however, these changes were found in the lumbar and cervical cords, medulla oblongata, cerebellum, and cerebrum. The degrees of intensity of the histopathologic changes in the lumbar and cervical cords were significantly higher than those in the medulla oblongata, cerebellum, and cerebrum.

Electron-microscopic Findings

Normal Neurons. Nerve cells vary in size and shape, and there are particularly great variations in the morphology of the nerve processes. Uninfected nerve cells show the usual cytoplasmic content including mitochondria, lipofuscin, and vacuoles. An ordered array of granular endoplasmic reticulum (Nissl substance) and Golgi packets are distributed fairly throughout the cytoplasm. Most nerve cells have a central spherical nucleus which varies in size.

Development of Cytopathogenesis and of Membrane-bound Vesicles in Infected Neurons. The changes in the neurons were distributed in the lumbar and cervical cords, medulla oblongata, pons, and thalamus on days

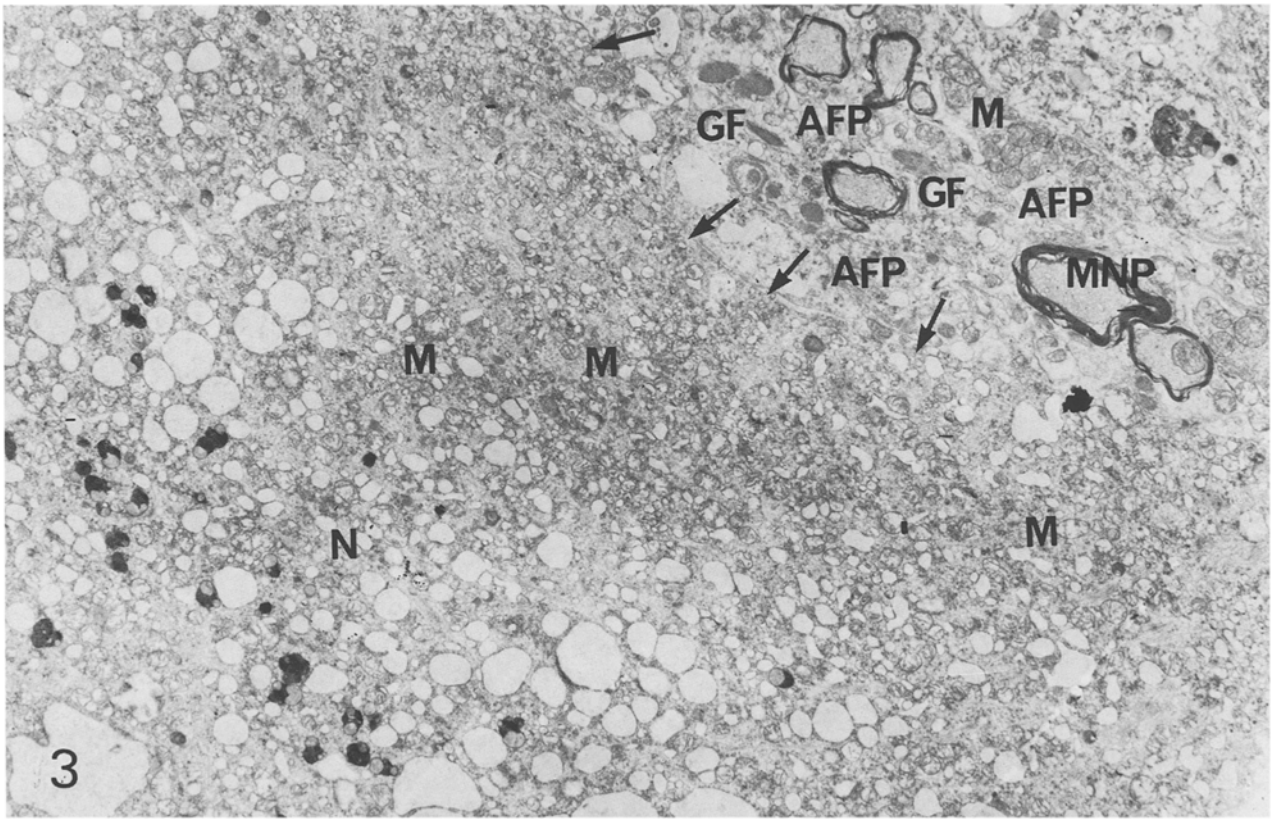

Fig. 3. A degenerating motoneuron (*N*) in the lumbar cord on day 3. Numerous cytoplasmic membrane-bound vesicles (*arrows*), degeneration or destruction of mitochondria (*M*), disappearance of Nissl substance or nucleus in a neuron. Note no abnormalities of astrocyte foot plates (*AFP*), glial filament (*GF*), and myelinated nerve processes (*MNP*) around a degenerating motoneuron. × 6,500

1 – 3 after infection. The lesions are prominent in the lumbar and cervical cords. Atrophy, degeneration, and disappearance of the nuclei were observed occasionally in damaged nerve cells. Numerous membrane-bound vesicles, disappearance or decrement of Nissl substance, and degeneration or destruction of mitochondria occurred in damaged neurons (Figs. 1, 3) and small or large membrane-bound vesicles, 500 – 800 Å in diameter, were found constantly. The structure of these vesicles was very similar to that in cultured CMK cells infected with poliovirus as shown in Figs. 6 and 7. In general, the vesicles of the periphery were larger than those in the central region. Each vesicle was limited by single or mutiple, closely apposed, smooth membranes. The number of membrane-bound vesicles increased with time after infection. As shown in Figs. 2 and 4, virus-like particles with a diameter of about 27 nm were found occasionally in these vesicles. Virus-like particles were also seen in the intracellular space associated with the membrane-bound vesicles. Intracytoplasmic crystals were not found in any of the neurons. Abnormalities were not observed in the astrocyte foot plates, the myelin and axon around damaged nerve cells as shown in Figs. 1 and 3. No poliovirus-like particles were found in astrocytes, oligodendrocytes, microglia (Hortega's cell), vascular endothelial or inflammatory cells, and macrophages in the lumbar and cervical cords, medulla oblongata, pons, and thalamus, although paracrystalline arrays of virus-like material were observed frequently in the cytoplasm of macrophages and vascular endothelial cells as seen in Fig. 11.

Normal CMK Cells. Uninfected CMK cells are large and spherical; their surface is provided with short microvilli. The nucleus is round or angular with several indentations. The cytoplasm is abundant containing a moderate amount of mitochondria, free ribosomes, and granular endoplasmic reticulum. The Golgi zone is prominent with numerous vesicles (Fig. 5).

Development of Cytopathogenesis and of Membrane-bound Vesicles in Infected CMK Cells. The rounding of CMK cells infected with poliovirus was first detected by electron microscopy at 5 h, and the cells became progressively more rounded with continued incubation. Disappearance of microvilli from the cytoplasmic membrane and atrophy, degeneration, or disappearance of the nuclei were found in most CMK cells at

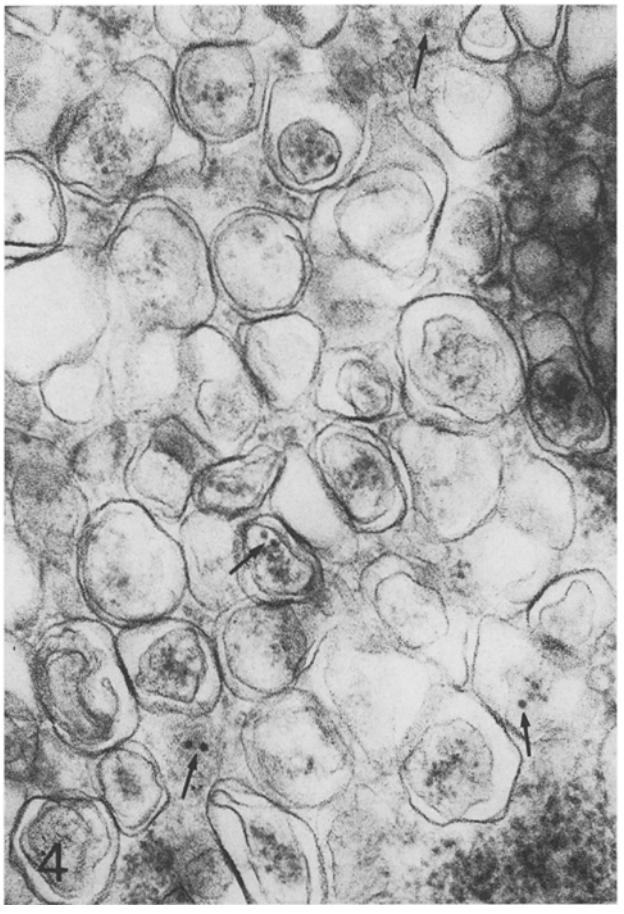

Fig. 4. Higher magnification of cytoplasmic membrane-bound vesicles in Fig. 3. Note virus-like particles (*arrows*) within or around the vesicles. ×62,500

5–24 h after infection. Membrane-bound vesicles, 500–1,800 Å in diameter, were detected in the cytoplasm 5–24 h after infection (Figs. 6, 7). The structure of these vesicles was very similar to those in damaged nerve cells infected with poliovirus as illustrated in Figs. 1–4. At these periods virus-like particles were scattered throughout the cytoplasm and were seen occasionally in membrane-bound vesicles (Figs. 7, 8); the cytoplasm of infected CMK cells also contained one or more well-defined virus crystalloids near the membrane-bound vesicles (Fig. 8).

Light-microscopic Peroxidase Studies

Virus antigen was not detected by staining with peroxidase-conjugated anti-rabbit gamma-globulin in the motoneurons of the lumbar and cervical cords of a monkey treated with normal rabbit serum prior to infection with poliovirus. In addition, virus antigen was not detected in the motoneurons of the lumbar and cervical cords in a monkey infected with enterovirus 71 stained with peroxidase-conjugated anti-rabbit gamma-globulin after treatment with anti-poliovirus rabbit serum.

The sections of the lumbar and cervical cords, cerebellum, and cerebrum of monkeys inoculated with poliovirus were stained with peroxidase-conjugated anti-rabbit gamma-globulin after treatment with anti-poliovirus rabbit serum. No virus antigen was detected in the nerve cells of the CNS of monkeys without clinical symptoms at 8 h and 1 day. In completely paralyzed monkeys on days 2 and 3, however, virus antigen was detected in the cytoplasm of degenerating or necrotic neurons of the anterior gray horns of the lumbar (Fig. 9) and cervical cords (Figs. 10), pons, and thalamus. No virus antigen was detected in either the glial, the inflammatory, or the vascular endothelial cells.

Discussion

In the present study, the occurrence of numerous membrane-bound vesicles and disappearance or decrement of Nissl substance and degeneration or destruction of mitochondria were noted usually in damaged motoneurons of the lumbar and cervical cords of monkeys infected with poliovirus on days 1–3 after infection. The structure of the vesicles in the cytoplasm of motoneurons was similar to that in infected cultured CMK cells. Virus-like particles were detected occasionally around or within the membrane-bound vesicles in the cytoplasm of the motoneurons and in cultured CMK cells, although intracytoplasmic crystals were not detected in any of the neurons. Bablamian et al. (1965) reported that in cell culture virus-specific protein synthesis is required for the production of viral pathogenesis. Our data suggest, therefore, that the formation of the membrane-bound vesicles is a reflection of cytopathogenic changes in the neurons.

In immunofluorescent studies, virus antigen was detected in the vascular endothelial and mononuclear inflammatory cells as well as motoneurons of the CNS in monkeys infected with poliovirus (Kovácks et al. 1963; Kanamitsu et al. 1967), and specific fluorescence was detected in the cytoplasm of motoneurons in the CNS of mice infected with the Lansing type 2 strain of poliovirus (Jubelt et al. 1970). On the contrary, Simon et al. (1970) reported that poliovirus antigen was not detected in the neurons, although antigen was found in the vascular endothelial and inflammatory cells. They suggested, therefore, that nerve cell damage is due to secondary effects of virus multiplication in the supporting cells of the CNS. In the present study, however, virus-like particles were not detected by electron microscopy in astrocytes, oligodendrocytes, microglia, vascular endothelial and inflammatory cells or mac-

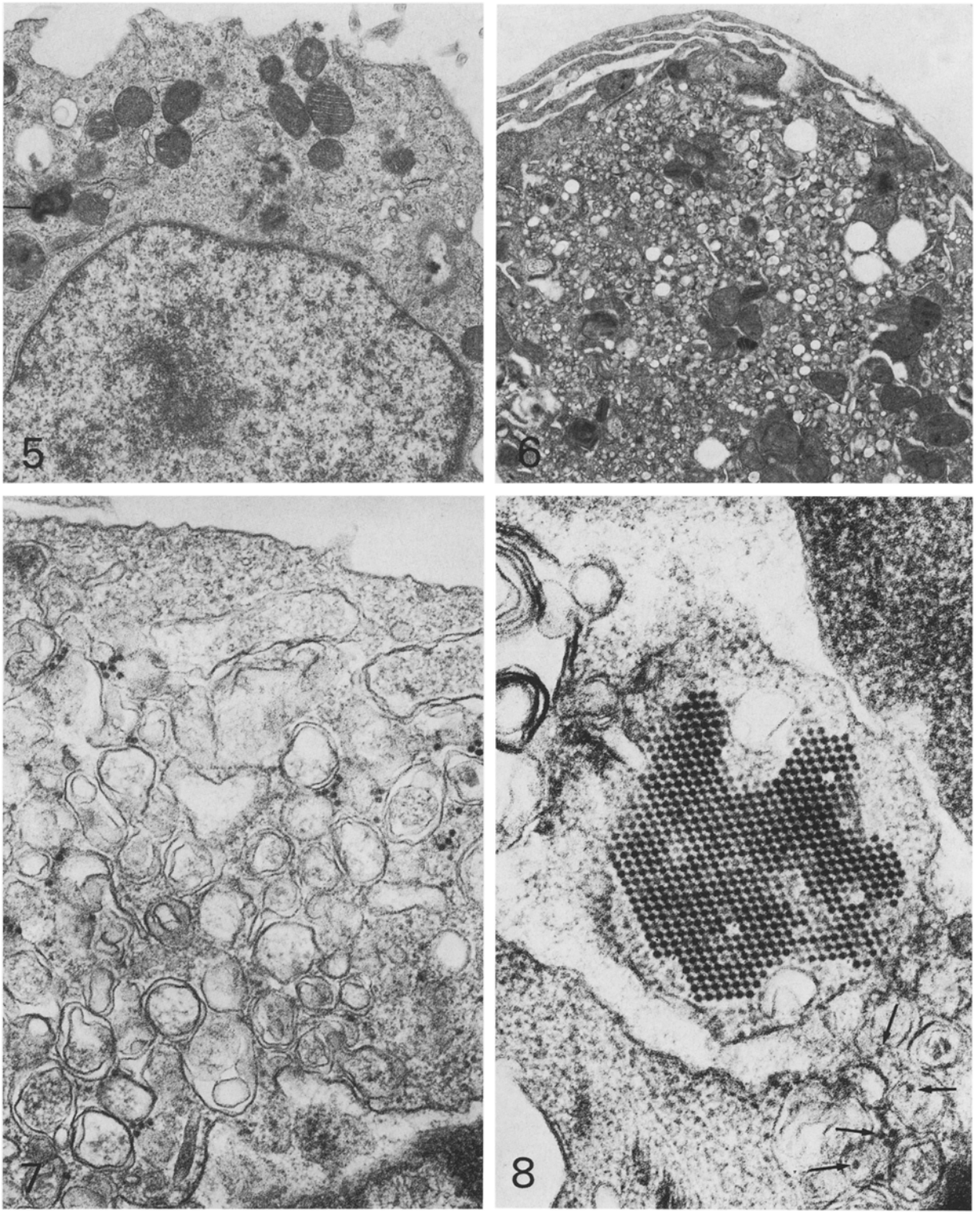

Fig. 5. An uninfected CMK cell incubated for 6 h showing usual cytoplasmic contents including a Golgi apparatus, mitochondria, and endoplasmic reticulum. Polyribosomes are scattered throughout the cytoplasm. ×12,500

Fig. 6. A CMK cell infected with poliovirus at 7 h. Note numerous cytoplasmic membrane-bound vesicles in a rounding cell. ×9,500

Fig. 7. Higher magnification of cytoplasmic membrane-bound vesicles in Fig. 6. Virus-like particles around the vesicles. ×62,500

Fig. 8. A CMK cell infected with poliovirus at 7 h. Intracytoplasmic crystal of poliovirus. Note virus-like particles within or around the membrane-bound vesicles at *bottom right* (*arrows*). ×77,500

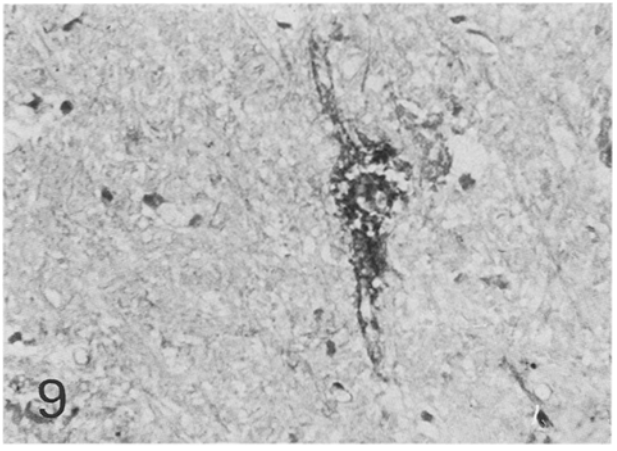

Fig. 9. The lumbar cord of a paralyzed monkey inoculated with poliovirus on day 3. Peroxidase antibody-stained section of anterior gray horn showing virus antigen in a degenerating motoneuron. × 200

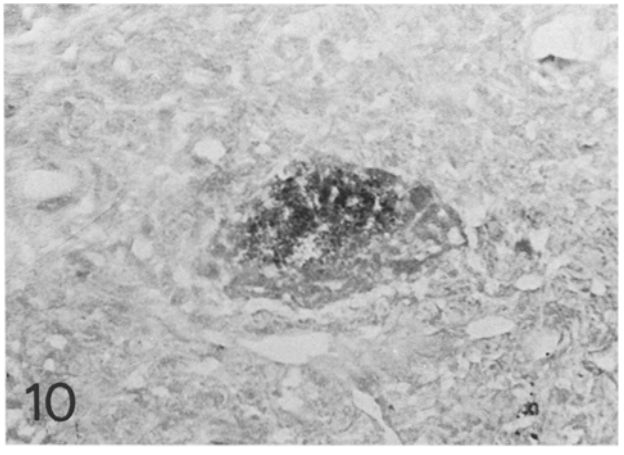

Fig. 10. The cervical cord of a paralyzed monkey inoculated with poliovirus on day 3. Peroxidase antibody-stained section of anterior gray horn showing virus antigen in a degenerating motoneurons. × 200

Fig. 11. A macrophage in the lumbar cord on day 3. Paracrystalline arrays of virus-like material surrounded by a membrane in the cytoplasm. No membrane-bound vesicle was found in any of the cytoplasms. × 50,000

rophages in the CNS of monkeys infected with poliovirus.

On the other hand, paracrystalline arrays of virus-like material were found frequently in the cytoplasm of macrophages and in the endothelial cells in the CNS of monkeys infected with poliovirus as illustrated in Fig. 11. Morphologically, the paracrystalline arrays of virus-like material in the cells were very similar to those in the cytoplasm and nucleus of a wide variety of cells as reported by many investigators (Fawcett and Burgos 1960; Harder and Swift 1969; Karasaki 1963; Wisniewski et al. 1972; Edmonds and Nagy 1973; Reimer et al. 1973; Tajima and Kudow 1976). The crystalline aggregates of poliovirus in the vascular endothelial and inflammatory cells reported by Blinzinger et al. (1968, 1969) were very similar to the paracrystalline arrays of virus-like material. The paracrystalline arrays of virus-like material were composed of regularly spaced laminae with an average diameter of 25 nm and were occasionally surrounded by a membrane as shown in Fig. 11. In the present study, however, no membrane was detected around the crystals of poliovirus in cultured CMK cells as seen in Fig. 8, although crystals were not found in the neurons of monkeys inoculated with poliovirus. We suppose, therefore, that the crystals of poliovirus in the vascular endothelial and inflammatory cells (Blinzinger et al. 1968, 1969) belong to the paracrystalline arrays of virus-like material. In this experiment, these paracrystalline arrays of virus-like material occurred most frequently in the cytoplasm of macrophages and vascular endothelial cells, where no indications of virus infection could be found. From these findings we suggest that these structures have nothing to do with the infection by poliovirus.

Poliovirus-like particles in the necrotizing motoneurons were first detected by Bodian (1964). In the present study, the crystalline aggregates of poliovirus, as indicated by Bodian, were occasionally found in the cytoplasm of degenerating motoneurons in the lumbar and cervical cords of monkeys infected with poliovirus. In higher magnification, however, these crystalline aggregates do not show the structure which is specific to poliovirus. The crystalline aggregates of poliovirus in necrotizing motoneurons of the CNS in monkeys infected with poliovirus as described by Bodian are very similar to aggregates of ribosomes. We suppose, therefore, that poliovirus particles (Bodian) may have much to do with aggregates of ribosomes. As mentioned above, virus-like particles were detected around or within the membrane-bound vesicles in the cytoplasm of motoneurons in the CNS of monkeys infected with poliovirus as well as infected cultured CMK cells. No virus particles or membrane-bound vesicles were found in astrocyte footplates, microglia, vascular endothelial and inflammatory cells. In addition, virus antigen was detected only in the nerve cells of the CNS by light-microscopic immunoperoxidase technique, although specific staining was never found in the supporting tissues or vascular endothelial and inflammatory cells. From the present results we suggest that the membrane-bound vesicles are very closely correlated with virus multiplication and that damage to the nerve cell is due to the direct action of virus multiplication.

Acknowledgements. We wish to express our thanks to Mr. I. Uchino, Dept. of Pathology, National Institute of Health, for his constant cooperation in the electron-microscopic study.

References

Bablamian R, Eggers HJ, Tamm I (1965) Studies on the mechanism of poliovirus-induced cell damage. II. The relation between poliovirus growth and virus-induced morphological changes in cells. Virology 26:114–121

Blinzinger K, Simon J, Magrath D, Boulger L (1968) Elektronenmikroskopische Beobachtungen bei experimenteller Poliomyelitis. Experientia 24:1095–1096

Blinzinger K, Simon J, Magrath D, Boulger L (1969) Poliovirus crystal within the endoplasmic reticulum of endothelial and mononuclear cell in the monkey spinal cord. Science 163:1336–1337

Bodian D (1964) An electron-microscopic study of the monkey spinal cord. III. Cytologic effects of poliovirus infection. Bull Johns Hopkins Hosp 114:21–119

Edmonds RH, Nagy F (1973) Crystalline inclusion bodies in the epididymis of the nine-banded armadillo. J Ultrastruct Res 42:82–86

Fawcett DW, Burgos MH (1960) Studies on the fine structure of the mammalian testis. II. The human interstitial tissue. Am J Anat 107:245–269

Hadek R, Swift HA (1960) A crystalloid inclusion in the rabbit blastocyst. J. Biophys Cytol 8:836–841

Jubelt B, Gallez-Hawaking G, Narayan O, Johnson RT (1970) Pathogenesis of human poliovirus infection in mice. 1. Clinical and pathological studies. J Neuropathol Exp Neurol 39:138–148

Kanamitsu K, Kasamaki A, Ogawa M, Kasahara S, Imamura M (1967) Immunofluorescent study on the pathogenesis of oral infection of poliovirus in monkeys. Jpn J Med Sci Biol 20:175–194

Karasaki S (1963) Studies on amphibian yolk. 1. The ultrastructure of the yolk platelet. J Cell Biol 18:135–166

Kovácks E, Baratawidjaja KK, Labzoffsky A (1963) Visualization of poliovirus type III in paraffin sections of monkeys spinal cord by indirect immunofluorescence. Nature 200:497–498

McLean IW, Nakane PK (1974) Periodate-lysine-paraformaldehyde fixative. A new fixative for immunoelectron microscopy. J Histochem Cytochem 22:1077–1083

Nakane PK, Pierce GB (1967) Enzyme-labeled antibody: Preparation and application for the localization of antigens. J Histochem Cytochem 14:929–931

Reimer L, Roessner A, Themann H, Bassewitz DBV (1973) Optical diffraction on tilting series of paracrystalline intranuclear inclusion of dog liver parenchymal cells. J Ultrastruct Res 45:356–365

Simon J, Magrath D, Boulger L (1970) The role of the defensive mechanism in experimental poliomyelitis. Prog Immunobiol Scand 4:643–649

Tajima M, Kudow S (1976) Morphology of the Warthin-Finkeldey giant cells in monkeys with experimentally induced measles. Acta Pathol Jpn 26:367–380

Wiśniewski H, Raine CS, Kay WJ (1972) Observations on viral demyelinating encephalomyelitis. Canine distemper. Lab Invest 26:589–599

Received July 29, 1983/Accepted February 20, 1984